

# Inhibition of ground-state superradiance and light-matter decoupling in circuit QED

Tuomas Jaako,<sup>1</sup> Ze-Liang Xiang,<sup>1</sup> Juan José Garcia-Ripoll,<sup>2</sup> and Peter Rabl<sup>1</sup>

<sup>1</sup>Vienna Center for Quantum Science and Technology,

Atominstitut, TU Wien, Stadionallee 2, 1020 Vienna, Austria

<sup>2</sup>Instituto de Física Fundamental, IFF-CSIC, Calle Serrano 113b, Madrid E-28006, Spain

(Dated: May 9, 2022)

We study effective light-matter interactions in a circuit QED system consisting of a single  $LC$  resonator, which is coupled symmetrically to multiple superconducting qubits. Starting from a minimal circuit model, we demonstrate that in addition to the usual collective qubit-photon coupling the resulting Hamiltonian contains direct qubit-qubit interactions, which prevent the otherwise expected superradiant phase transition in the ground state of this system. Moreover, these qubit-qubit interactions are responsible for an opposite mechanism, which at very strong couplings completely decouples the photon mode and projects the qubits into a highly entangled ground state. These findings shed new light on the controversy over the existence of superradiant phase transitions in cavity and circuit QED systems, and show that the physics of ultrastrong light-matter interactions in two- or multi-qubit settings differ drastically from the more familiar one qubit case.

PACS numbers: 42.50.Pq, 05.30.Rt, 85.25.-j

The Dicke model (DM) is frequently used in atomic and solid-state systems as a minimal model to describe phenomena related to the collective coupling of many emitters to a single radiation mode [1, 2]. When extended to the ultrastrong coupling regime, the ground state of the DM undergoes a phase transition into a superradiant state [3, 4, 10], where the atoms are polarized and the field mode exhibits a non-vanishing expectation value. While this phenomenon has been observed with engineered Dicke Hamiltonians in driven cold atom systems [6–8], the existence of a superradiant phase transition (SRT) in the ground state of equilibrium cavity QED systems is still subject of ongoing debates [9–13]. This question has regained considerable interest with the development of circuit QED systems [2, 14, 15, 17], where ultrastrong light-matter interactions between superconducting two level systems and microwave photons have recently been implemented [6, 7, 18, 19]. In particular, it has been argued [22] that the equivalent of the so-called  $A^2$  term—which supposedly prevents the SRT in atomic systems [9]—does not play a crucial role in these artificial circuit QED devices. However, these predictions have been questioned on very general grounds [23] and a full resolution of this matter remains open.

In this work we investigate a circuit QED system, where  $N$  charge qubits are coupled symmetrically to a single microwave mode, such that in the limit of weak couplings the system reduces to the standard DM. However, the full Hamiltonian for such a system necessarily contains additional direct qubit-qubit interactions, which have been ignored in many previous studies, but become non-negligible as one approaches the ultrastrong coupling regime. We find that these qubit-qubit interactions—rather than an  $A^2$ -like term—prevent the conventional SRT in this circuit QED system to occur. Instead, with increasing coupling the system gradually evolves into a

hybridized qubit-photon state, but without broken symmetry. Surprisingly, at even higher interaction strengths, an opposite effect can take place, where the photonic component of the ground state completely decouples, while the qubits collapse into a highly entangled Dicke state with vanishing dipole moment. We provide a simple theoretical description to explain this and other interesting properties of such interacting Dicke models in the ultrastrong coupling regime. These findings are experimentally accessible with state-of-the-art superconducting devices, but also provide new insights for closely related effects discussed in the optical or THz regime [11, 12, 24].

*Model.*—We consider a superconducting circuit as depicted in Fig. 1 a), where  $N$  charge qubits [17, 25] are coupled symmetrically to a single mode lumped element resonator with capacitance  $C_r$  and inductance  $L_r$ . Each qubit is represented by a Cooper pair box with capacitance  $C_q$  and Josephson energy  $E_J$  and coupled to the LC resonator via an additional capacitance  $C_g$ . The whole circuit is described by the Lagrangian

$$\mathcal{L} = \frac{C_r \dot{\Phi}_r^2}{2} - \frac{\Phi_r^2}{2L_r} + \sum_{i=1}^N \left[ \mathcal{L}_q(\Phi_i, \dot{\Phi}_i) + \frac{C_g}{2} (\dot{\Phi}_r - \dot{\Phi}_i)^2 \right], \quad (1)$$

where  $\Phi_\eta(t) = \int_{-\infty}^t V_\eta(s)ds$  is the generalized flux [1] associated with the voltage  $V_\eta$  at each node,  $\eta = r, 1, \dots, N$  [see Fig. 1 a)]. The Lagrangian for each qubit is  $\mathcal{L}_q(\Phi, \dot{\Phi}) = C_q(\dot{\Phi} - V_G)^2/2 + E_J \cos(\Phi/\Phi_0)$ , where  $V_G$  is the applied gate voltage and  $\Phi_0 = \hbar/(2e)$  is the reduced flux quantum. Following the standard quantization procedure we replace the  $\Phi_\eta$  and the conjugate node charges  $Q_\eta = \partial \mathcal{L} / \partial \dot{\Phi}_\eta$  by operators obeying  $[\Phi_\eta, Q_{\eta'}] = i\hbar \delta_{\eta\eta'}$ . For the resulting circuit Hamiltonian we then obtain [27]

$$H = \frac{Q_r^2}{2\bar{C}_r} + \frac{\Phi_r^2}{2L_r} + \sum_{i=1}^N \left[ H_q^i + \frac{Q_r \mathcal{Q}_i}{\bar{C}_g} \right] + \sum_{i \neq j} \frac{\mathcal{Q}_i \mathcal{Q}_j}{2\bar{C}_{qq}}, \quad (2)$$

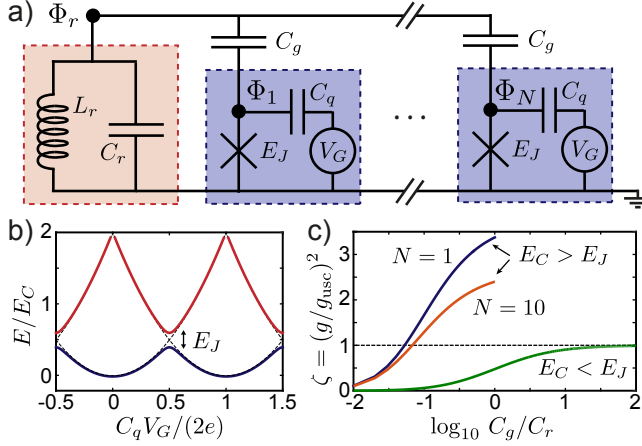


FIG. 1. (color online). a) Circuit model for  $N$  charge qubits coupled to a single lumped-element resonator. b) Sketch of the energy levels of a single charge qubit as a function of the applied gate voltage and for  $E_C \gg E_J$ . c) Plot of the coupling parameter  $\zeta = (g/g_{usc})^2$  as a function of  $C_g/C_r$  and a specific set of circuit parameters  $C_r = 10 \text{ fF}$ ,  $C_q = 0.5 \text{ fF}$ , and  $L_r = 1 \text{ nH}$ . For the two upper lines  $E_J/h = 2 \text{ GHz}$  and the condition  $E_J/E_C < 1$  is fulfilled over the whole range of plotted values. The lowest line represents the transmon limit ( $E_J/E_C > 1$ ) given in Eq. (4) for  $N = 1$ .

where  $\mathcal{Q}_i = Q_i + C_q V_G$  is the displaced charge and  $H_q^i = \mathcal{Q}_i^2/(2\bar{C}_q) - E_J \cos(\Phi_i/\Phi_0)$  the Hamiltonian for an individual qubit. The capacitances are  $\bar{C}_r = \bar{C}^2/(C_q + C_g)$ ,  $\bar{C}_q = \bar{C}^2/[C_r + C_g + (N-1)C_g C_q/(C_q + C_g)]$ ,  $\bar{C}_g = \bar{C}^2/C_g$ ,  $\bar{C}_{qq} = (C_g + C_q)\bar{C}^2/C_g^2$  and  $\bar{C}^2 = C_g C_r + C_q(C_r + N C_g)$ .

Equation (2) first of all shows that the coupling of individual qubits to a common resonator mode renormalizes the bare resonator and qubit energies. This is analogous to the effect of the  $A^2$ -term [9], which in atomic cavity QED systems increases the photonic field energy. Interestingly, here the coupling *lowers* the charging energies, i.e.,  $\bar{C}_{r,q} > C_{r,q}$ , which is exactly the opposite effect and would at first sight favor a SRT. However, from the last term in Eq. (2) we also see that the Legendre transformation from voltage to charge variables introduces additional direct qubit-qubit interactions, the effect of which we analyze in the following.

In a final step we express  $Q_r = Q_0^r(a^\dagger + a)$  and  $\Phi_r = iQ_0^r/(\bar{C}_r\bar{\omega}_r)(a^\dagger - a)$  in terms of annihilation and creation operators,  $a$  and  $a^\dagger$ , where  $\bar{\omega}_r = 1/\sqrt{L_r\bar{C}_r}$  and  $Q_0^r = \sqrt{\hbar\bar{C}_r\bar{\omega}_r/2}$ . We further restrict each qubit to the two lowest states  $|0\rangle$  and  $|1\rangle$  (at this stage without further justification), which are separated by an energy  $\hbar\bar{\omega}_q$ . For the examples considered below we can then write  $H_q^i \simeq \hbar\bar{\omega}_q\sigma_z^i/2$  and  $\mathcal{Q}_i \simeq Q_0^q\sigma_x^i$ , where  $Q_0^q = \langle 1|\mathcal{Q}|0\rangle$  and the  $\sigma_k$  are the usual Pauli operators. Under these assumptions and by introducing collective spin operators  $S_k = \frac{1}{2}\sum_i \sigma_k^i$ , we finally obtain ( $\hbar = 1$ )

$$H \simeq \bar{\omega}_r a^\dagger a + \bar{\omega}_q S_z + g(a^\dagger + a)S_x + D S_x^2, \quad (3)$$

where  $g = 2Q_0^r Q_0^q/(\hbar\bar{C}_g)$  and  $D = 2(Q_0^q)^2/(\hbar\bar{C}_{qq})$ . In the absence of the last term, Eq. (3) reduces to the standard DM, which exhibits a superradiant ground state for couplings  $\sqrt{N}g \geq g_{usc}$  [10], where we use  $g_{usc} = \sqrt{\bar{\omega}_r\bar{\omega}_q}$  to define the onset of the ultrastrong coupling regime for a single qubit.

*Ultrastrong coupling and no-go theorems.*—To proceed it is instructive to evaluate the value of the single-qubit coupling parameter  $\zeta = (g/g_{usc})^2$  that can actually be achieved with a given circuit design. We first do so for the frequently used transmon qubit [29], which is operated in the regime  $E_J \gg E_C = e^2/(2\bar{C}_q)$  and  $V_G = 0$ . In this case the two lowest eigenstates are well approximated by harmonic oscillator states with  $\bar{\omega}_q \simeq \sqrt{8E_C E_J}$  and  $Q_0^q \simeq \sqrt{\hbar\bar{C}_q\bar{\omega}_q/2}$  and we obtain

$$\zeta = \frac{C_g^2}{C_r(C_g + C_q) + C_g(C_g + NC_q)} < 1. \quad (4)$$

This shows that independently of the circuit parameters the single-qubit ultrastrong coupling regime cannot be reached. Such a limit on the coupling parameter is consistent with more general no-go theorems discussed in Ref. [23], and can be traced back to the fact that in harmonic or weakly nonlinear systems the coupling  $g \sim \sqrt{\bar{\omega}_q\bar{\omega}_r}$  is directly related to the qubit and the resonator frequency. To break this relation we now consider instead the charge qubit limit  $E_J \ll E_C$  and  $C_q V_G/(2e) = 1/2$  [see Fig. 1 b)]. In this case  $Q_0^q \approx e$  is approximately independent of  $\bar{\omega}_q \simeq E_J$  and we obtain

$$\zeta = \frac{4C_g^2}{C_r(C_g + C_q) + C_g(C_g + NC_q)} \times \frac{E_C}{E_J}. \quad (5)$$

Therefore, while in practice there might be additional constraints on the achievable parameters, there is no fundamental limit that prevents one from reaching the ultrastrong coupling regime even for a single qubit, for example, by simply lowering  $E_J$ . This is explicitly shown in Fig. 1 c) for a concrete set of realistic parameters and in agreement with many previously analyzed circuits [3–5] based on the highly nonlinear flux qubit design [8, 17].

Let us return to the full circuit QED Hamiltonian (3). Note that for  $N \gg 1$  neither Eq. (4) nor Eq. (5) prevents one from reaching the collective ultrastrong coupling regime,  $N\zeta > 1$ , but now the additional qubit-qubit interactions  $\sim D$  must be taken into account. Following the standard approach [10], we first consider the limit  $N \gg 1$ , and use the Holstein-Primakoff approximation to replace spins by harmonic operators, i.e.  $S_z \rightarrow b^\dagger b - N/2$  and  $S_x \rightarrow \sqrt{N}(b + b^\dagger)/2$ , where  $[b, b^\dagger] = 1$ . In this case we obtain the quadratic Hamiltonian

$$H_{\text{HP}} = \bar{\omega}_c a^\dagger a + \bar{\omega}_q b^\dagger b + G(a + a^\dagger)(b^\dagger + b) + D_N(b + b^\dagger)^2, \quad (6)$$

where  $G = g\sqrt{N}/2$  and  $D_N = ND/4$ . This Hamiltonian can be diagonalized by a Bogoliubov transformation [10,

[24, 27, 28], from which we obtain the two eigenmode frequencies

$$\omega_{\pm}^2 = \frac{1}{2} \left[ \bar{\omega}_r^2 + \Omega_q^2 \pm \sqrt{(\bar{\omega}_r^2 - \Omega_q^2)^2 + 16G^2\bar{\omega}_r\bar{\omega}_q} \right], \quad (7)$$

where  $\Omega_q^2 = \bar{\omega}_q(\bar{\omega}_q + 4D_N)$ . The SRT occurs, when the ground state of  $H_{\text{HP}}$  becomes unstable, i.e., when  $\omega_-$  vanishes. This requires  $G^2 > \bar{\omega}_c\Omega_q/4$ , or equivalently,  $N(g^2/\bar{\omega}_r) > ND + \bar{\omega}_q$ , and for  $D = 0$  we recover the usual transition point mentioned above. However, in view of the relation  $\bar{C}_{qq} = \bar{C}_g^2/\bar{C}_r$  in Eq. (2), the qubit-qubit interaction strength and the qubit-resonator coupling are not independent and by writing

$$D = \frac{g^2}{\bar{\omega}_r} + \delta, \quad (8)$$

we obtain  $\delta = 0$  current model and  $\delta \geq 0$  for other equivalent circuit designs [27]. This means that also in the present circuit QED setup a SRT in the conventional sense does not occur, and it is prevented by a mechanism, which is analogous to the effect of dipole-dipole interactions in intersubband polariton systems [24, 28]. Since this effect is absent for a single qubit, there is a fundamental difference between single- and multi-qubit cavity QED settings, which does not follow from otherwise closely related studies of the  $A^2$ -term [9, 22, 23].

*Light-matter decoupling.*—Having established the absence of a SRT in the linearized regime, we are now interested in the actual ground state of Hamiltonian (3) under the constraint (8) and  $\delta \geq 0$ , but for otherwise arbitrary coupling parameters. In Fig. 2 a) and b) we plot the expectation values of the mean photon number  $\langle a^\dagger a \rangle$  and the spin expectation values  $\langle S_z \rangle$  and  $\langle S_x^2 \rangle$  as a function of the coupling  $g$  and for  $N = 9$  and  $N = 10$  qubits. The plot shows a gradual increase of the photon number, which—as expected from the analysis above—varies smoothly across the SRT point  $g = \sqrt{\bar{\omega}_r\bar{\omega}_q}/N$ . This behavior can be fully understood from the linearized Hamilton  $H_{\text{HP}}$ , from which we derive the approximate initial scaling [27]

$$\langle a^\dagger a \rangle \simeq \frac{Ng^2\bar{\omega}_q}{4(\bar{\omega}_r + \bar{\omega}_q)^2[\bar{\omega}_q + N(D - g^2/\bar{\omega}_r)]}. \quad (9)$$

The validity of these results requires a low excited-state population of each individual qubit, i.e.  $g \ll \bar{\omega}_r + \bar{\omega}_q$ . Beyond this point nonlinear effects start to play a significant role and surprisingly, for an even number of qubits we observe a sudden decrease of the photon number and  $\lim_{g \rightarrow \infty} \langle a^\dagger a \rangle = 0$ . At the same time the qubits remain in a highly excited state, i.e.  $\langle S_z \rangle \approx 0$ , with a vanishing polarization along  $x$ , i.e.  $\langle S_x \rangle, \langle S_x^2 \rangle \rightarrow 0$ . In Fig. 2 c) we also plot the entanglement entropy,  $S_E(\rho) = -\text{Tr}\{\rho \log_2(\rho)\}$ , for the reduced qubit density operator and for the density operator of a single qubit. It shows that while the spin and cavity subsystems become decoupled at large  $g$ , the qubits remain highly entangled among themselves.

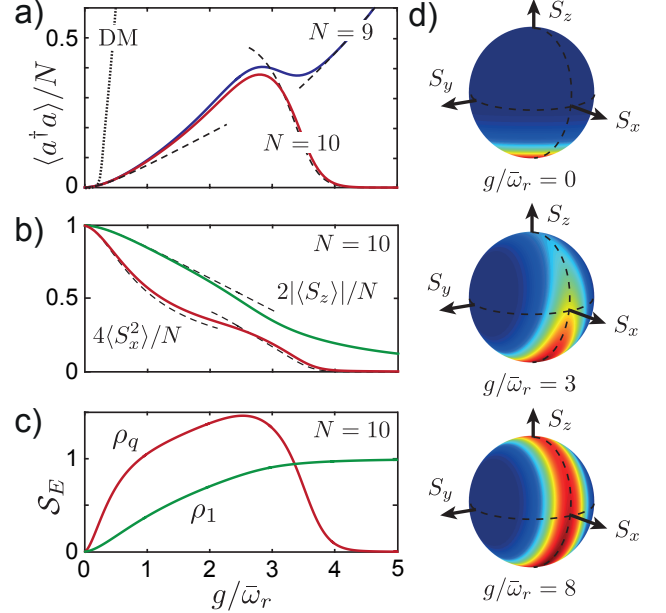


FIG. 2. (color online). Ground-state expectation values of a) the photon number and b) the collective spin operators as a function of the coupling  $g$ . The dotted line indicates the prediction from the Dicke model (DM) and the dashed lines the results obtained from  $H_{\text{HP}}$  in Eq. (6) and  $H_{\text{eff}}$  in Eq. (11) in the weak and strong coupling limit, respectively. c) Entanglement entropy  $S_E(\rho) = -\text{Tr}\{\rho \log_2(\rho)\}$  in the ground state  $|G\rangle$  of Hamiltonian (3) evaluated for the reduced density matrix of the qubit subsystem,  $\rho_q = \text{Tr}\{|G\rangle\langle G|\}$ , and for the reduced density matrix of a single qubit,  $\rho_1 = \text{Tr}_{N-1}\{\rho_q\}$ . d) Plot of the Q-function  $Q(\vec{n}) = \langle \vec{n} | \rho_q | \vec{n} \rangle$ , where  $\vec{n}$  is a unit vector on the Bloch sphere and  $|\vec{n}\rangle$  is the corresponding coherent spin state. Note that in b)-d) only the results for  $N = 10$  are shown and for all plots  $\bar{\omega}_q/\bar{\omega}_r = 0.5$  and  $\delta = 0$  have been assumed.

We remark that related light-matter decoupling mechanisms have recently been described in extended multimode systems [12, 34]. There the inclusion of  $A^2$ -like terms expels the relevant field modes from the coupling region, an effect which can already be described within a linearized model. In the present single-mode setup such a mechanism is not possible, and the above observations already indicate that here the field decoupling is a highly nonlinear and nonclassical effect. A heuristic explanation for this behavior can be obtained by considering the limit  $D \gg g, \bar{\omega}_{r,q}$ , where the qubit-qubit interaction is the dominant energy and therefore favors the state  $|m_x = 0\rangle$ , where  $S_x|m_x\rangle = m_x|m_x\rangle$ , as the ground state. Since the coupling to the field  $\sim S_x$ , it then also vanishes and the resonator mode decouples. This is visualized in Fig. 2 d), in terms of the Q-function of the reduced qubit state on the Bloch sphere, which approaches a circle in the  $x = 0$  plane for large  $g$ . For odd  $N$ , there is no  $m_x = 0$  state, which explains why this decoupling mechanism does not take place for the example of  $N = 9$  qubits.

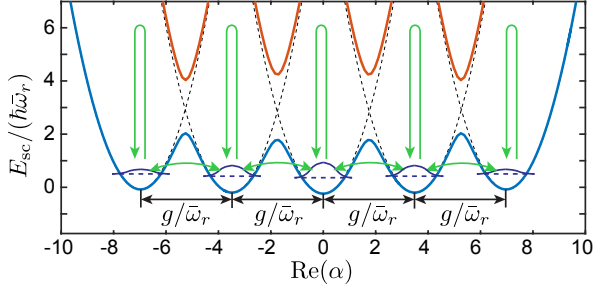


FIG. 3. (color online). Plot of the lowest two energy levels  $E_{\text{sc}}$  obtained from the diagonalization of the semiclassical qubit Hamiltonian  $H_{\text{sc}}(\alpha) = \langle \alpha | H | \alpha \rangle$ , and for  $g/\bar{\omega}_r = 3.5$ ,  $\bar{\omega}_q/\bar{\omega}_r = 1$  and  $N = 4$ . The arrows indicate first and second order processes induced by  $H_1 = \bar{\omega}_q S_z$  on the otherwise degenerate ground state manifold.

Let us now develop a more precise description of the system in the regime  $g/\bar{\omega}_r > 1$ . We write  $H = H_0 + H_1$ , where  $H_1 = \bar{\omega}_q S_z$ . The first term,  $H_0$ , commutes with  $S_x$  and can be diagonalized exactly,  $H_0 |\Psi_{s,m_x,n}\rangle = E_{m_x,n} |\Psi_{s,m_x,n}\rangle$  [27]. Here

$$|\Psi_{s,m_x,n}\rangle = e^{-\frac{g}{\bar{\omega}_r}(a^\dagger - a)S_x} |s, m_x\rangle |n\rangle, \quad (10)$$

where  $|n\rangle$  are photon number states and  $|s, m_x\rangle$  are collective spin states of given total spin  $s = 0, \dots, N/2$  and projection quantum number  $m_x = -s, \dots, s$ . Therefore, the eigenstates of  $H_0$  are harmonic oscillator states, which are displaced by an amount  $m_x g/\bar{\omega}_r$ . The corresponding energies are  $E_{m_x,n} = \delta m_x^2 + \bar{\omega}_r n$ , showing that for  $\delta \rightarrow 0$ , each  $n$ -manifold contains a set of  $2^N$  degenerate states. The energy penalty from the  $S_x^2$ -term is exactly compensated by a lowering of the interaction energy when the resonator mode is displaced. This is illustrated in Fig. 3, where we plot the lowest two eigenvalues of the semiclassical qubit Hamiltonian,  $H_{\text{sc}}(\alpha) = \langle \alpha | H | \alpha \rangle$ , for  $s = N/2$ . The energies  $E_{\text{sc}}(\alpha)$  can be interpreted as Born-Oppenheimer potentials for a classical resonator with amplitude  $\alpha$ .

To model the low energy properties of  $H$  we now focus on the ground state manifold,  $n = 0$ , and include quantum corrections due to  $H_1$ . This term first of all couples neighboring  $m_x$  levels within this manifold, i.e.,  $\langle \Psi_{s,m_x,0} | S_z | \Psi_{s,m_x \pm 1,0} \rangle = e^{-g^2/2\bar{\omega}_r^2} \langle s, m_x | S_z | s, m_x \pm 1 \rangle$ . In addition,  $H_1$  also couples to states in energetically higher manifolds,  $n > 0$ . This effect can be treated in second order perturbation theory and predominately leads to an energy shift  $\sim [m_x^2 - s(s+1)]\bar{\omega}_q^2\bar{\omega}_r/(2g^2)$ . This shift singles out the  $s = N/2$  states as the lowest energy manifold and by defining operators  $\tilde{S}_k$  via the relation  $\langle \Psi_{s,m'_x,0} | \tilde{S}_k | \Psi_{s,m_x,0} \rangle = \langle s, m'_x | S_k | s, m_x \rangle$ , we obtain within this manifold the effective collective spin Hamil-

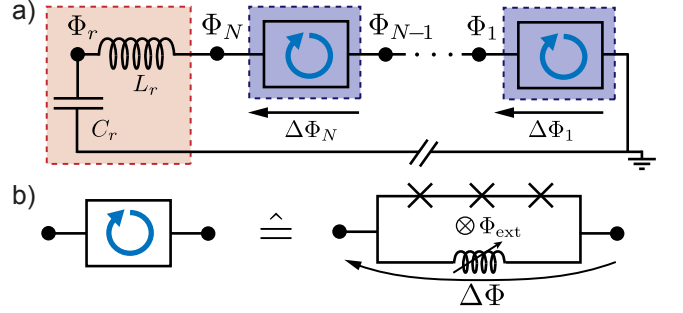


FIG. 4. (color online). Circuit model for a collective QED system with inductively coupled flux qubits. When expressed in terms of the flux across each qubit,  $\Delta\Phi_i = \Phi_i - \Phi_{i-1}$ , the magnetic energy  $(\Phi_r - \sum \Delta\Phi_i)^2/(2L_r)$  associated with the inductance  $L_r$  leads to qubit-resonator as well as qubit-qubit interactions, with the same relation  $D = g^2/\bar{\omega}_r$  as in the charge qubit case. b) Specific realization of a flux qubit based on the design used in Refs. [6, 7] to reach the ultrastrong coupling regime. For more details see [27].

tonian [27]

$$H_{\text{eff}} \simeq \left( \delta + \frac{\bar{\omega}_q^2 \bar{\omega}_r}{2g^2} \right) \tilde{S}_x^2 + \bar{\omega}_q e^{-g^2/2\bar{\omega}_r^2} \tilde{S}_z. \quad (11)$$

From this model we immediately see that for  $g/\bar{\omega}_r \gg 1$  the coupling to neighboring  $m_x$  states is exponentially suppressed and for even  $N$  the ground state is indeed  $|G\rangle = |\Psi_{N/2,m_x=0,n=0}\rangle$  with a vanishing photon number. By taking into account first order corrections to states  $|\Psi_{N/2,m_x=\pm 1,n=0}\rangle$  we obtain the approximate scalings

$$\langle a^\dagger a \rangle \approx \frac{N(N+2)g^6}{2\bar{\omega}_r^4 \bar{\omega}_q^2} e^{-g^2/\bar{\omega}_r^2}, \quad \Delta E \approx \frac{\bar{\omega}_r \bar{\omega}_q^2}{2g^2}, \quad (12)$$

where  $\Delta E = E_1 - E_0$  is the gap between the ground and the first excited state. Note that this non-exponential closing of the energy gap is very atypical for qubit-resonator models in the ultrastrong coupling regime. For an odd number of qubits there is no  $m_x = 0$  state and the ground state is  $|G\rangle \simeq (|\Psi_{N/2,m_x=-1/2,n=0}\rangle + |\Psi_{N/2,m_x=1/2,n=0}\rangle)/\sqrt{2}$  and  $\langle a^\dagger a \rangle \simeq g^2/(4\bar{\omega}_r^2)$  simply increases in the large  $g$  limit. The next higher state is the corresponding antisymmetric superposition and therefore the energy splitting now exhibits the usual exponential scaling, i.e.,  $\Delta E \simeq (N/2+1)\bar{\omega}_q e^{-g^2/2\bar{\omega}_r^2}$ . Although for certain quantities the admixture of higher  $n$ -levels must be taken into account [27], we find that within its range of validity,  $\sqrt{s(s+1)g^2/(\bar{\omega}_r \bar{\omega}_q)} \lesssim 1$  and  $g/\bar{\omega} \gtrsim 1$ , the effective model  $H_{\text{eff}}$  provides an accurate description of the low energy properties of an ultrastrongly coupled collective circuit QED system.

*Conclusions.*—In summary, we have analyzed collective interactions in circuit QED systems in the ultrastrong coupling regime. Going beyond the previously described  $A^2$  corrections, we have shown that the more

important qubit-qubit interactions prevent a SRT in such systems and lead instead to light-matter decoupling and highly entangled ground states at very strong interactions. Note that our results derived here for charge qubits extend immediately to equivalent setups using flux qubits inductively coupled to zero-mode resonators as illustrated in Fig. 4. Using the tuneability of the coupling [5–7] in these setups, it should be possible to dynamically test our predictions for  $N = 2$  or more qubits, over a wide range of coupling strengths, including the scaling of the qubit-qubit interaction strength, light-matter decoupling and ground state properties.

*Acknowledgments.*—We thank J. Majer and S. Putz for stimulating discussions. This work was supported by the Austrian Science Fund (FWF) through SFB FO-QUS F40, DK CoQuS W 1210 and the START grant Y 591-N16 and by the European Commission through the FP7/ITC Project SIQS (600645) and the Marie Skłodowska-Curie Grant IF 657788. J.J.G.R. acknowledges support from the Spanish Mineco Project FIS2012-33022 and the CAM Research Network QUITEMAD+.

---

[1] R. H. Dicke, Coherence in Spontaneous Radiation Processes, *Phys. Rev.* **93**, 99 (1954).

[2] T. Brandes, Coherent and collective quantum optical effects in mesoscopic systems, *Physics Reports* **408**, 315 (2005).

[3] K. Hepp and E. H. Lieb, On the superradiant phase transition for molecules in a quantized radiation field: the dicke maser model, *Ann. Phys.* **76**, 360 (1973).

[4] Y. K. Wang and F. T. Hioe, Phase Transition in the Dicke Model of Superradiance, *Phys. Rev. A* **7**, 831 (1973).

[5] C. Emary and T. Brandes, Chaos and the quantum phase transition in the Dicke model, *Phys. Rev. E* **67**, 066203 (2003).

[6] K. Baumann, C. Guerlin, F. Brennecke, and T. Esslinger, Dicke quantum phase transition with a superfluid gas in an optical cavity, *Nature* **464**, 1301 (2010).

[7] M. P. Baden, K. J. Arnold, A. L. Grimsmo, S. Parkins, M. D. Barrett, Realization of the Dicke Model Using Cavity-Assisted Raman Transitions, *Phys. Rev. Lett.* **113**, 020408 (2014).

[8] J. Klinder, H. Keßler, M. Wolke, L. Mathey, and A. Hemmerich, Dynamical phase transition in the open Dicke model, *PNAS* **112**, 3290 (2015).

[9] K. Rzazewski, K. Wodkiewicz, and W. Zakowicz, Phase Transitions, Two-Level Atoms, and the  $A^2$  Term, *Phys. Rev. Lett.* **35**, 432 (1975).

[10] J. M. Knight, Y. Aharonov, and G. T. C. Hsieh, Are super-radiant phase transitions possible?, *Phys. Rev. A* **17**, 1454 (1978).

[11] J. Keeling, Coulomb interactions, gauge invariance, and phase transitions of the Dicke model, *J. Phys: Cond. Mat.* **19**, 295213 (2007).

[12] S. De Liberato, Light-Matter Decoupling in the Deep Strong Coupling Regime: The Breakdown of the Purcell Effect, *Phys. Rev. Lett.* **112**, 016401 (2014).

[13] A. Vukics, T. Griesser, and P. Domokos, Elimination of the  $A$ -Square Problem from Cavity QED, *Phys. Rev. Lett.* **112**, 073601 (2014).

[14] A. Blais, R. S. Huang, A. Wallraff, S. M. Girvin, and R. J. Schoelkopf, Cavity quantum electrodynamics for superconducting electrical circuits: An architecture for quantum computation, *Phys. Rev. A* **69**, 062320 (2004).

[15] A. Wallraff, D. I. Schuster, A. Blais, L. Frunzio, R. S. Huang, J. Majer, S. Kumar, S. M. Girvin, and R. J. Schoelkopf, Strong coupling of a single photon to a superconducting qubit using circuit quantum electrodynamics, *Nature (London)* **431**, 162 (2004).

[16] M. H. Devoret, S. Girvin, and R. Schoelkopf, Circuit-QED: How strong can the coupling between a Josephson junction atom and a transmission line resonator be?, *Ann. Phys. (NY)* **16**, 767 (2007).

[17] J. Q. You and F. Nori, Atomic physics and quantum optics using superconducting circuits, *Nature (London)* **474**, 589 (2011).

[18] T. Niemczyk, *et al.*, Circuit quantum electrodynamics in the ultrastrong-coupling regime, *Nature Phys.* **6**, 772 (2010).

[19] P. Forn-Diaz, J. Lisenfeld, D. Marcos, J. J. Garcia-Ripoll, E. Solano, C. J. P. M. Harmans, and J. E. Mooij, Observation of the Bloch-Siegert Shift in a Qubit-Oscillator System in the Ultrastrong Coupling Regime, *Phys. Rev. Lett.* **105**, 237001 (2010).

[20] F. Yoshihara, T. Fuse, S. Ashhab, K. Kakuyanagi, S. Saito, and K. Semb, arXiv:1602.00415 (2016).

[21] P. Forn-Diaz, J. J. Garcia-Ripoll, B. Peropadre, M. A. Yurtalan, J.-L. Orgiazzi, R. Belyansky, C. M. Wilson, and A. Lupascu, arXiv:1602.00416 (2016).

[22] P. Nataf and C. Ciuti, No-go theorem for superradiant quantum phase transitions in cavity QED and counterexample in circuit QED, *Nature Commun.* **1**, 72 (2010).

[23] O. Viehmann, J. von Delft, and F. Marquardt, Superradiant Phase Transitions and the Standard Description of Circuit QED, *Phys. Rev. Lett.* **107**, 113602 (2011).

[24] Y. Todorov and C. Sirtori, Few-Electron Ultrastrong Light-Matter Coupling in a Quantum LC Circuit, *Phys. Rev. X* **4**, 041031 (2014).

[25] Y. Makhlin, G. Schön, and A. Shnirman, Quantum-state engineering with Josephson-junction devices, *Rev. Mod. Phys.* **73**, 357 (2001).

[26] M. H. Devoret, *Quantum Fluctuations in Electrical Circuits, Les Houches, Session LXIII*, (1997).

[27] See the supplemental material for more detailed derivations of the main results presented.

[28] Y. Todorov, A. M. Andrews, R. Colombelli, S. De Liberato, C. Ciuti, P. Klang, G. Strasser, and C. Sirtori, Ultrastrong Light-Matter Coupling Regime with Polariton Dots, *Phys. Rev. Lett.* **105**, 196402 (2010).

[29] J. Koch, T. M. Yu, J. Gambetta, A. A. Houck, D. I. Schuster, J. Majer, A. Blais, M. H. Devoret, S. M. Girvin, and R. J. Schoelkopf, Charge-insensitive qubit design derived from the Cooper pair box, *Phys. Rev. A* **76**, 042319 (2007).

[30] J. Bourassa, J. M. Gambetta, A. A. Abdumalikov, O. Astafiev, Y. Nakamura, and A. Blais, Ultrastrong coupling regime of cavity QED with phase-biased flux qubits, *Phys. Rev. A* **80**, 032109 (2009).

[31] P. Nataf and C. Ciuti, Vacuum Degeneracy of a Circuit QED System in the Ultrastrong Coupling Regime, *Phys. Rev. Lett.* **104**, 023601 (2010).

- [32] B. Peropadre, D. Zueco, D. Porras, and J. J. Garcia-Ripoll, Nonequilibrium and Nonperturbative Dynamics of Ultrastrong Coupling in Open Lines, *Phys. Rev. Lett.* **111**, 243602 (2013).
- [33] T. P. Orlando, J. E. Mooij, L. Tian, C. H. van der Wal, L. S. Levitov, S. Lloyd, and J. J. Mazo, Superconducting persistent-current qubit, *Phys. Rev. B* **60**, 15398 (1999).
- [34] M. Malekakhlagh and H. E. Türeci, Origin and implications of an  $A^2$ -like contribution in the quantization of circuit-QED systems, *Phys. Rev. A* **93**, 012120 (2016).

## Supplemental material for: Inhibition of ground-state superradiance and light-matter decoupling in circuit QED

This supplemental material contains additional details on the model and the derivation of various results stated in the main part of the paper.

### CIRCUIT MODELS

In this Section we outline in more detail the derivation of the collective cavity Hamiltonian  $H$  given in Eq. (3) in the main text. We first do so for the charge qubit setup discussed already in the paper, and then show in a second step, how an equivalent model can be derived from a circuit based on flux qubits.

#### Capacitively coupled charge qubits

Let us consider the circuit shown in Fig. 1 a) in the main text, where  $N$  identical charge qubits are capacitively coupled to a single  $LC$ -resonator via a coupling capacitance  $C_g$ . For each qubit the voltage  $V_i$  on the island and the voltage  $V_r$  across the resonator capacitance can be chosen independently and the circuit can be described in terms of the associated generalized flux variables [S1]

$$\Phi_\eta(t) = \int_{-\infty}^t ds V_\eta(s), \quad \eta = r, 1, \dots, N. \quad (\text{S1})$$

The capacitive energy of the circuit is given by

$$T = \frac{C_r \dot{\Phi}_r}{2} + \sum_{k=1}^N \frac{C_q \dot{\Phi}_k}{2} + \sum_{k=1}^N \frac{C_g \left( \dot{\Phi}_k - \dot{\Phi}_r \right)^2}{2} + \sum_{k=1}^N \frac{C_q \left( \dot{\Phi}_k - V_G \right)^2}{2} \quad (\text{S2})$$

$$= \frac{1}{2} \dot{\Phi}^T \mathcal{C} \dot{\Phi} - \dot{\Phi}^T \mathbf{a} + \frac{NC_q V_G^2}{2}, \quad (\text{S3})$$

where  $\dot{\Phi} = \left( \dot{\Phi}_r, \dot{\Phi}_1, \dots, \dot{\Phi}_N \right)^T$ ,  $\mathbf{a} = (0, C_q V_G, \dots, C_q V_G)^T$  and

$$\mathcal{C} = \begin{pmatrix} C_r + NC_g & -C_g & -C_g & \dots & -C_g \\ -C_g & C_q + C_g & 0 & \dots & 0 \\ -C_g & 0 & C_q + C_g & \dots & 0 \\ \vdots & \vdots & \vdots & \ddots & \vdots \\ -C_g & 0 & 0 & \dots & C_q + C_g \end{pmatrix} \quad (\text{S4})$$

is the capacitance matrix. The inductive energy is

$$V = \frac{\Phi_r^2}{2L_r} - \sum_{k=1}^N E_J \cos \left( \frac{\Phi_k}{\Phi_0} \right), \quad (\text{S5})$$

where  $\Phi_0 = \hbar/(2e)$  is the reduced flux quantum. The Lagrangian is the sum of the above capacitive and inductive energies  $\mathcal{L} = T - V$ . The conjugate node charges  $Q_\eta = \partial \mathcal{L} / \partial \dot{\Phi}_\eta$  can be written in a compact form as

$$\mathbf{Q} = \frac{\partial \mathcal{L}}{\partial \dot{\Phi}} = \mathcal{C} \dot{\Phi} - \mathbf{a}, \quad (\text{S6})$$

where  $\mathbf{Q} = (Q_r, Q_1, \dots, Q_N)^T$ . The Hamiltonian function is obtained from the Lagrangian via a Legendre transformation, i.e.  $\mathcal{H} = \mathbf{Q}^T \dot{\Phi} - \mathcal{L}$ , which can be written in vector notation as

$$\mathcal{H} = \frac{1}{2} (\mathbf{Q} + \mathbf{a})^T \mathcal{C}^{-1} (\mathbf{Q} + \mathbf{a}) + V. \quad (\text{S7})$$

To quantize  $\mathcal{H}$  to the Hamiltonian operator  $H$  we replace the node fluxes  $\Phi_\eta$  and charges  $Q_\eta$  with operators, and impose the canonical commutation relation  $[\Phi_\eta, Q_{\eta'}] = i\hbar\delta_{\eta\eta'}$ . The inverse of the capacitance matrix is

$$\frac{1}{C} = \frac{1}{\bar{C}^2} \begin{pmatrix} C_g + C_q & C_g & C_g & \dots & C_g \\ C_g & X & Y & \dots & Y \\ C_g & Y & X & \dots & Y \\ \vdots & \vdots & \vdots & \ddots & \vdots \\ C_g & Y & Y & \dots & X \end{pmatrix} \quad (\text{S8})$$

where  $\bar{C}^2 = C_r C_q + C_g (C_r + N C_q)$  and we used the abbreviations

$$X = C_r + C_g + (N - 1) \frac{C_g C_q}{(C_g + C_q)}, \quad Y = \frac{C_g^2}{(C_g + C_q)}. \quad (\text{S9})$$

The resulting Hamiltonian can then be written in the form

$$H \equiv H_r + H_q + H_g + H_{qq}, \quad (\text{S10})$$

where the individual parts are given by

$$H_r = \frac{Q_r^2}{2\bar{C}_r} + \frac{\Phi_r^2}{2L_r}, \quad (\text{S11})$$

$$H_q = \sum_{k=1}^N \frac{(Q_k + C_q V_G)^2}{2\bar{C}_q} - E_J \cos\left(\frac{\Phi_k}{\Phi_0}\right), \quad (\text{S12})$$

$$H_g = \frac{Q_r}{\bar{C}_g} \sum_{k=1}^N (Q_k + C_q V_G), \quad (\text{S13})$$

$$H_{qq} = \sum_{k,l=1, l \neq k}^N \frac{(Q_k + C_q V_G)(Q_l + C_q V_G)}{2\bar{C}_{qq}}. \quad (\text{S14})$$

With the notation introduced above the capacitances are given by  $\bar{C}_r^{-1} = (C_g + C_q)/\bar{C}^2$ ,  $\bar{C}_q^{-1} = X/\bar{C}^2$ ,  $\bar{C}_g^{-1} = C_g/\bar{C}^2$ ,  $\bar{C}_{qq}^{-1} = Y/\bar{C}^2 = \bar{C}_r/\bar{C}_g^2$ . Finally, by defining  $Q_k = Q_k + C_q V_G$  we obtain the result given in Eq. (2) of the main text.

By expressing the resonator variables in terms of annihilation and creation operators and using a two level approximation for the qubit Hamiltonian we obtain

$$H = \hbar\bar{\omega}_r a^\dagger a + \frac{\hbar\bar{\omega}_q}{2} \sum_{k=1}^N \sigma_z^k + \frac{\hbar g}{2} \sum_{k=1}^N (a^\dagger + a) \sigma_x^i + \frac{\hbar D}{4} \sum_{k,l=1}^N \sigma_x^k \sigma_x^l, \quad (\text{S15})$$

where  $\bar{\omega}_r = 1/\sqrt{L_r \bar{C}_r}$ ,  $\hbar\bar{\omega}_q$  is the splitting of the qubit energy levels,  $\hbar g = 2Q_0^r Q_0^q/(\bar{C}_g)$  and  $\hbar D = 2(Q_0^q)^2/(\bar{C}_{qq})$ . Note that here we have added a constant energy shift  $\hbar D N/4 = \hbar D/4 \sum_k (\sigma_x^k)^2$ , such that the indices in the last term of Eq. (S15) run over all qubits. Since  $\bar{C}_{qq} = \bar{C}_r/\bar{C}_g^2$  we can write

$$\hbar D = \frac{2(Q_0^q)^2 \bar{C}_r}{C_g^2} = \frac{(2Q_0^q)^2 \bar{\omega}_r \bar{C}_r}{2C_g^2 \bar{\omega}_r} = \frac{\hbar g^2}{\bar{\omega}_r}. \quad (\text{S16})$$

Using the collective spin operators  $S_\alpha = \frac{1}{2} \sum_{k=1}^N \sigma_\alpha^k$ ,  $\alpha = x, y, z$ , we obtain Eq. (3) in the main text.

#### Transmon regime

We consider the transmon regime  $E_J \gg E_C$ , where  $E_C = e^2/(2\bar{C}_q)$ . In this regime the qubits behave as weakly non-linear harmonic oscillators and we can choose  $V_G = 0$ . The splitting of the qubit states is given by the frequency of the oscillator,  $\hbar\bar{\omega}_q = \sqrt{8E_c E_J}$ , and  $Q_0^q = \sqrt{\hbar\bar{\omega}_q C_g}/2$ . For the single-qubit coupling parameter we then obtain

$$\left(\frac{g}{g_{\text{usc}}}\right)^2 = \frac{4\hbar^2 \bar{\omega}_r \bar{\omega}_q \bar{C}_r \bar{C}_q}{4\hbar^2 \bar{\omega}_r \bar{\omega}_q \bar{C}_g} = \frac{\bar{C}_r \bar{C}_q}{\bar{C}_g^2} = \frac{C_g^2}{C_r(C_g + C_q) + C_g(C_g + N C_q)} < 1, \quad (\text{S17})$$

which is the result stated in Eq. (4) in the main text.

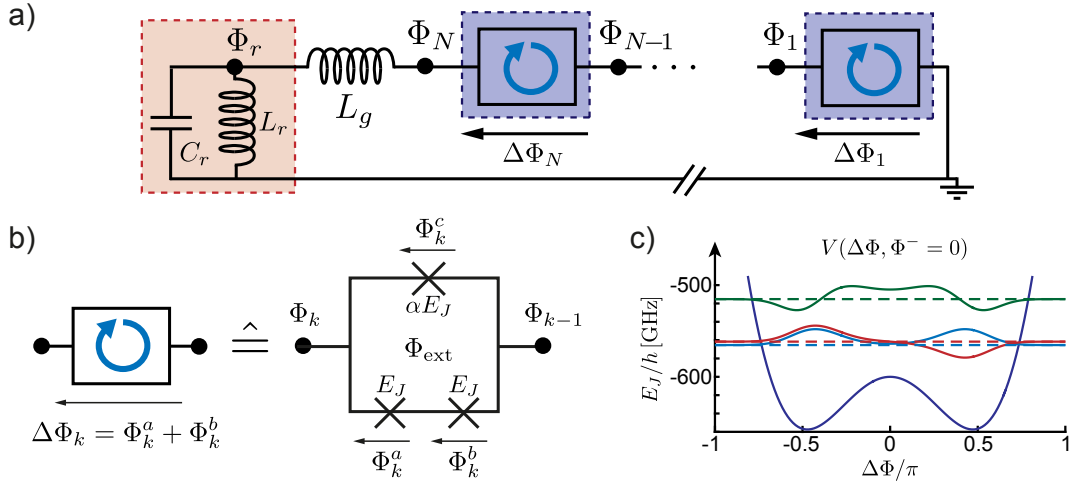


FIG. S1. a) Circuit model for a collective cavity QED system with  $N$  flux qubits coupled via an inductance  $L_g$  to an LC resonator. Compared to Fig. 4 in the main text, here the resonator inductance  $L_r$  and the coupling inductance  $L_g$  can be chosen independently. b) Specific realization of a flux qubit based on three Josephson junctions. The capacitance  $C_\alpha$  in parallel to the upper junction and the capacitances  $C$  in parallel to each of the lower junctions are not shown. c) Potential of a three junction flux qubit as a function of the variable  $\Delta\Phi$  and for the parameters given in the text. The dashes lines indicate the energies of the three lowest qubit states and the corresponding wavefunctions. Note that these energies include the energy offset from the confining potential along the  $\Phi^-$  direction and therefore they appear above the potential barrier.

#### Charge qubit regime

Let us now consider the charge regime  $E_C \gg E_J$ , where the charging energy dominates over the Josephson energy. In this situation one usually operates the qubits at the charge degeneracy point  $C_q V_G / (2e) = 1/2$ . In this regime and using the two-level approximation we have  $\hbar\bar{\omega}_q = E_J$  and  $Q_0^q = e$ . Comparing the coupling strength  $g$  to the system frequencies gives

$$\left(\frac{g}{g_{usc}}\right)^2 = \frac{4e^2\hbar\bar{\omega}_r\bar{C}_r}{2\bar{C}_g^2\hbar\bar{\omega}_rE_J} = \frac{1}{E_J} \frac{4\bar{C}_r\bar{C}_q}{\bar{C}_g^2} \frac{e^2}{2\bar{C}_q} = \frac{4C_g^2}{C_r(C_g + C_q) + C_g(C_g + NC_q)} \frac{E_C}{E_J}. \quad (\text{S18})$$

We have gained a factor of  $4E_C/E_J$  compared to the transmon case. Note that  $E_C$  itself decreases with increasing coupling capacitance, but as shown in Fig. 1 c) in the main text a set of parameters can be found where a single qubit can reach the ultrastrong coupling regime.

Apart from the coupling parameter  $(g/g_{usc})^2$ , which can in principle always be increased by reducing the qubit frequency, another relevant parameter is the ratio  $g/\bar{\omega}_r$ . For this quantity we obtain

$$\frac{g}{\bar{\omega}_r} = \frac{2e}{\hbar\bar{\omega}_r\bar{C}_g} \sqrt{\frac{\hbar\bar{\omega}_r\bar{C}_r}{2}} = \sqrt{\frac{16\pi^2he^2\bar{\omega}_r\bar{C}_r}{4\pi\hbar^2\bar{\omega}_r^2\bar{C}_g^2}} = 2\sqrt{\pi} \sqrt{\frac{C_g^2C_r}{(C_q + C_g)\bar{C}^2}} \sqrt{\frac{Z_r}{R_K}}, \quad (\text{S19})$$

where  $Z_r = \sqrt{L_r/C_r}$  is the impedance of the bare  $LC$ -resonator and  $R_K = h/e^2 \approx 26 \text{ k}\Omega$  is the von Klitzing constant (resistance quantum). Thus, obtaining  $g \sim \bar{\omega}_r$  requires  $LC$  circuits with an impedance that is much higher than the most frequently used  $Z_r \approx 50 \Omega$ . The scaling  $\sqrt{Z_r/R_K}$  for a capacitively coupled qubit has been previously pointed out in Ref. [S2].

#### Flux-coupled qubits

Figure 4 in the main texts shows an equivalent circuit QED system, where  $N$  flux qubits are coupled inductively to a lumped element LC resonator. In previous works [S2–S5] it has already been pointed out that such an inductive coupling scheme can lead to very strong qubit-resonator interactions. Indeed, using this strategy the ultrastrong coupling regime has been recently demonstrated experimentally [S6, S7] with a single qubit.

To be slightly more general we analyze here the circuit shown in Fig. S1 a), where the resonator inductance  $L_r$  is independent of the coupling inductance  $L_g$ . For now we leave the details of each flux qubit unspecified, and simply denote by  $\Delta\Phi_k = \Phi_k - \Phi_{k-1}$  the flux difference across each qubit. Thus,  $\Phi_N = \sum_k \Delta\Phi_k$  and the Lagrangian for the whole circuit can be written as

$$\mathcal{L} = \frac{C_r \dot{\Phi}_r^2}{2} - \frac{\Phi_r^2}{2L_r} + \frac{\left(\Phi_r - \sum_{k=1}^N \Delta\Phi_k\right)^2}{2L_g} + \sum_{k=1}^N \mathcal{L}_{FQ}^k. \quad (\text{S20})$$

Here  $\mathcal{L}_{FQ}^k$  is the Lagrangian for a single flux qubit, which depends on  $\Delta\Phi_k$ , but in general also on additional degrees of freedom. Since there is no capacitive coupling between the resonator and the qubits, the derivation of the corresponding Hamilton operator is straight forward and we obtain

$$H = H_r + \sum_{k=1}^N \bar{H}_{FQ}^k + H_g + H_{qq}, \quad (\text{S21})$$

where the individual terms are given by

$$H_r = \frac{Q_r^2}{2C_r} + \frac{\Phi_r^2}{2\bar{L}_r}, \quad (\text{S22})$$

$$\bar{H}_{FQ}^k = H_{FQ}^k + \frac{\Delta\Phi_k^2}{2L_g}, \quad (\text{S23})$$

$$H_g = -\frac{\Phi_r}{L_g} \sum_{k=1}^N \Delta\Phi_k, \quad (\text{S24})$$

$$H_{qq} = \sum_{k,l=1, k \neq l}^N \frac{\Delta\Phi_k \Delta\Phi_l}{2L_g}. \quad (\text{S25})$$

Here we have defined the effective inductance of the resonator  $\bar{L}_r = L_r L_g / (L_r + L_g)$  and  $H_{FQ}^k$  is the bare Hamiltonian of the  $k$ th flux qubit in the absence of the resonator. Note that in contrast to the capacitive coupling scheme, here the inductive coupling introduces a positive energy contribution (i.e. a positive  $A^2$ -term) for the resonator and each qubit. However, this correction does not scale with the number of qubits,  $N$ , and therefore it does not prevent the system from reaching the ultrastrong coupling regime.

Before we discuss a specific flux qubit design, let us simply assume that the qubit dynamics is restricted to the two lowest eigenstates  $|0\rangle$  and  $|1\rangle$  of  $\bar{H}_{FQ}$ , which are separated by an energy  $\hbar\bar{\omega}_q$ . In this case the Hamiltonian reduces to the same form as given above in Eq. (S15) with

$$\hbar g = \frac{2\Phi_q^0 \Phi_r^0}{L_g}, \quad \hbar D = \frac{2(\Phi_q^0)^2}{L_g}, \quad (\text{S26})$$

where  $\Phi_0^r = \sqrt{\hbar/(2C_r\bar{\omega}_r)}$  and  $\Phi_q^0 = \langle 0 | \Delta\Phi | 1 \rangle$ . By rewriting the qubit-qubit interaction strength we see that

$$\hbar D = \frac{\hbar g^2}{\bar{\omega}_r} \frac{\hbar\bar{\omega}_r L_g}{2(\Phi_r^0)^2} = \frac{\hbar g^2}{\bar{\omega}_r} \frac{L_g}{\bar{L}_r} = \frac{\hbar g^2}{\bar{\omega}_r} \left(1 + \frac{L_g}{L_r}\right) = \frac{\hbar g^2}{\bar{\omega}_r} + \delta. \quad (\text{S27})$$

Therefore, for this more general circuit we obtain a finite  $\delta \geq 0$ , which vanishes as  $L_r \rightarrow \infty$  (corresponding to the circuit shown in Fig. 4 in the main text).

#### *Limits to the coupling strength*

Let us first consider the limit of a weakly non-linear qubit, where we can again assume that the lowest qubits states are well described by a quadratic Hamiltonian

$$\bar{H}_{FQ}^k \approx \frac{Q_q^2}{2C_q} + \frac{\Phi_r^2}{2\bar{L}_q}, \quad (\text{S28})$$

where  $\bar{L}_q = L_q L_g / (L_q + L_g)$  and  $C_q$  and  $L_q$  are the capacitance and the linear inductance of the bare qubit circuit, respectively. Then,  $\Phi_q^0 = \sqrt{\hbar / (2\bar{\omega}_q C_q)}$ , where  $\bar{\omega}_q = \sqrt{1 / (C_q \bar{L}_q)}$  and

$$\frac{g^2}{\bar{\omega}_r \bar{\omega}_q} = \frac{4}{2\bar{\omega}_r C_r 2\bar{\omega}_q C_q L_g^2 \bar{\omega}_r \bar{\omega}_q} = \frac{C_r \bar{L}_r C_q \bar{L}_q}{C_r C_q L_g^2} = \frac{L_r L_q}{(L_r + L_g)(L_q + L_g)} < 1. \quad (\text{S29})$$

Again we see that in this weakly nonlinear regime the single-qubit ultrastrong coupling regime cannot be reached. As we describe below, in a highly nonlinear flux qubit design the matrix element  $\varphi_q^0 = \Phi_q^0 / \Phi_0 \approx \pi/2$  is approximately independent of the qubit frequency and we obtain

$$\frac{g^2}{\bar{\omega}_r \bar{\omega}_q} = \frac{4(\varphi_q^0)^2 \Phi_0^2}{\hbar L_g^2 2\bar{\omega}_r C_r \bar{\omega}_r \bar{\omega}_q} = \left( \frac{\Phi_0^2 / L_g}{\hbar \omega_q} \right) \frac{2(\varphi_q^0)^2 \bar{L}_r}{L_g} = 2(\varphi_q^0)^2 \left( \frac{\Phi_0^2 / L_g}{\hbar \omega_q} \right) \frac{L_r}{L_r + L_g}. \quad (\text{S30})$$

Therefore, compared to the linear regime we gain a factor, which is roughly given by the ratio of the inductive energy of the coupling inductance and the qubit level splitting. For this regime we can also compute the ratio  $g / \bar{\omega}_r$ ,

$$\frac{g}{\bar{\omega}_r} = \frac{4\Phi_0 \varphi_q^0}{\sqrt{2\hbar C_r \bar{\omega}_r^3 L_g}} = \frac{\varphi_q^0}{\sqrt{\pi}} \sqrt{\frac{R_K \sqrt{C_r \bar{L}_r}}{L_g^2}} = \frac{\varphi_q^0}{\sqrt{\pi}} 4 \sqrt{\frac{L_r}{L_g} \left( \frac{L_r}{L_r + L_g} \right)^3 \sqrt{\frac{R_K}{Z_r}}}. \quad (\text{S31})$$

In this situation the ratio is proportional to  $\sqrt{R_K / Z_r}$  on the contrary to the charge coupling case where we obtained  $\sqrt{Z_r / R_K}$ . The use of inductive couplings is thus more favorable to reach the ultrastrong coupling regime, which, again, has already been pointed out in Ref. [S2].

#### Example: Three-junction flux qubit

While the analysis above applies to various different flux qubit designs, we here illustrate the experimental feasibility of such a circuit for a basic flux qubit composed of three Josephson junctions [S8], as shown in Fig. S1 b). The qubits have two identical junctions  $E_J$  and one junction with Josephson energy  $\alpha E_J$ . For each flux qubit we denote by  $\Phi_k^c$  the phase difference across the junction  $\alpha E_J$  and by  $\Phi_k^a$  and  $\Phi_k^b$  the phase jumps across the other two junctions [see Fig. S1 b)]. Then we define  $\Delta\Phi_k = \Phi_k^a + \Phi_k^b$  and  $\Phi_k^- = \Phi_k^a - \Phi_k^b$ . The fluxes  $\Delta\Phi_k$  and  $\Phi_k^c$  are related by the flux quantization condition  $\Delta\Phi_k - \Phi_k^c + \Phi_{\text{ext}} = 0$ , where  $\Phi_{\text{ext}}$  is the external flux through each loop. With these definitions the capacitive energy of qubit  $k$  reads

$$T_k = \frac{\alpha C(\Delta\dot{\Phi}_k)^2}{2} + \frac{C(\Delta\dot{\Phi}_k + \dot{\Phi}_k^-)^2 / 4}{2} + \frac{C(\Delta\dot{\Phi}_k - \dot{\Phi}_k^-)^2 / 4}{2} = \frac{C_q \Delta\dot{\Phi}_k^2}{2} + \frac{C_- (\Delta\dot{\Phi}_k^-)^2}{2}, \quad (\text{S32})$$

where  $C_q = C(\alpha + 1/2)$  and  $C_- = C/2$  are the effective capacitances. The inductive energy becomes

$$V_k = -E_J \left[ \cos \left( \frac{\Delta\Phi_k + \Phi_k^-}{2\Phi_0} \right) + \cos \left( \frac{\Delta\Phi_k - \Phi_k^-}{2\Phi_0} \right) + \alpha \cos \left( \frac{\Delta\Phi_k + \Phi_{\text{ext}}}{\Phi_0} \right) \right] \quad (\text{S33})$$

$$= -E_J \left[ 2 \cos \left( \frac{\Delta\Phi_k}{2\Phi_0} \right) \cos \left( \frac{\Phi_k^-}{2\Phi_0} \right) + \alpha \cos \left( \frac{\Delta\Phi_k + \Phi_{\text{ext}}}{\Phi_0} \right) \right]. \quad (\text{S34})$$

The Lagrangian of the  $k$ th qubit is then given by  $\mathcal{L}_{FQ}^k = T_k - V_k$  and one obtains the Hamiltonian by the normal quantization procedure. After including the correction term from the coupling to the resonator the modified qubit Hamiltonian is given by

$$\bar{H}_{FQ}^k = \frac{Q_k^2}{2C_q} + \frac{(Q_k^-)^2}{2C_-} - E_J \left[ 2 \cos \left( \frac{\Delta\Phi_k}{2\Phi_0} \right) \cos \left( \frac{\Phi_k^-}{2\Phi_0} \right) + \alpha \cos \left( \frac{\Delta\Phi_k + \Phi_{\text{ext}}}{\Phi_0} \right) \right] + \frac{(\Delta\Phi_k)^2}{2L_g}, \quad (\text{S35})$$

where the conjugate charges are  $Q_k = \partial\mathcal{L}/\partial(\Delta\dot{\Phi}_k)$  and  $Q_k^- = \partial\mathcal{L}/\partial(\dot{\Phi}_k^-)$ .

We see that the potential energy has a minimum for  $\Phi^- = 0$ , while for  $\Phi_{\text{ext}}/\Phi_0 = \pi$  it exhibits a double-well structure for the variable  $\Delta\Phi$ . This is shown in Fig. S1 c) for a realistic set of parameters,  $L_g = 4\text{nH}$ ,  $C = 4\text{fF}$ ,  $E_J/h = 500\text{GHz}$  and  $\alpha = 0.8$ . For this example the lowest two qubit state are the symmetric and antisymmetric superposition of the ground states in the left and right potential well, which are separated by a tunnel splitting of  $\bar{\omega}_q/(2\pi) \approx 3.75\text{GHz}$ . At the same time the next level is split by  $\Delta E_{32} \approx 46.4\text{GHz}$ , such that a two level approximation is justified. By choosing the resonator parameters as  $L_r = 4\text{nH}$ , and  $Z = \sqrt{L_r/C_r} = 50\Omega$  we obtain  $\omega_r/(2\pi) \approx 3.98\text{GHz}$ ,  $\bar{\omega}_q/\bar{\omega}_r \approx 0.94$ . This demonstrates the possibility of reaching the ultrastrong coupling regime,  $g/\bar{\omega}_r \approx 2.15$  and  $g^2/(\bar{\omega}_r \bar{\omega}_q) \approx 4.91$ , with this basic qubit design. More elaborate multi-junction designs can be used to achieve a tuneable coupling as described in Refs. [S6, S7].

### HOLSTEIN-PRIMAKOFF APPROXIMATION

Let us consider the effective Hamiltonian describing both coupling schemes considered above,

$$H = \hbar\bar{\omega}_r a^\dagger a + \hbar\bar{\omega}_q S_z + \hbar g(a^\dagger + a)S_x + \hbar D S_x^2. \quad (\text{S36})$$

If the couplings  $g$  and  $D$  are sufficiently weak, the ground state of this Hamiltonian is simply given by the state where all the qubits are in the ground state and the resonator is in a vacuum state. By using the Holstein-Primakoff transformation [S9, S10] the collective spin operators  $S_\pm = S_x \pm iS_y$  and  $S_z$  can be written in terms of bosonic operators  $b$  and  $b^\dagger$  as

$$S_+ = b^\dagger \sqrt{N - b^\dagger b}, \quad (\text{S37})$$

$$S_- = \sqrt{N - b^\dagger b} b, \quad (\text{S38})$$

$$S_z = \left( b^\dagger b - \frac{N}{2} \right). \quad (\text{S39})$$

Under the assumption that  $N \gg 1$  and the total number of excitations remains small, i.e.  $\langle b^\dagger b \rangle / N \ll 1$  we can approximate

$$S_x \simeq \sqrt{N}(b^\dagger + b)/2, \quad (\text{S40})$$

and we obtain the quadratic Hamiltonian

$$H_{\text{HP}} = \hbar\bar{\omega}_r a^\dagger a + \hbar\bar{\omega}_q b^\dagger b + \hbar G(a^\dagger + a)(b^\dagger + b) + \hbar D_N(b^\dagger + b)^2, \quad (\text{S41})$$

where  $\hbar G = \sqrt{N}g/2$  is the collective coupling strength and  $D_N = ND/4$ . This Hamiltonian can be diagonalized and written as [S10]

$$H_{\text{HP}} = \sum_{\alpha=\pm} \hbar\omega_\alpha c_\alpha^\dagger c_\alpha, \quad (\text{S42})$$

where the excitation frequencies are given by

$$\omega_\pm^2 = \frac{1}{2} \left[ \bar{\omega}_r^2 + \Omega_q^2 \pm \sqrt{(\bar{\omega}_r^2 - \Omega_q^2)^2 + 16G^2\bar{\omega}_r\bar{\omega}_q} \right] \quad (\text{S43})$$

and  $\Omega_q^2 = \bar{\omega}_q(\bar{\omega}_q + 4D_N)$ . As described in the main text, by using the relation  $D = g^2/\bar{\omega}_r + \delta$  we find that both excitation frequencies are positive as long as  $\delta \geq 0$  and  $\bar{\omega}_q > 0$ .

The ground state  $|G\rangle$  of this Hamiltonian is characterized by  $c_\pm|G\rangle = 0$ . Using this property we can calculate the average photon number in the ground state. We obtain

$$\langle a^\dagger a \rangle = \frac{\cos(2\theta) A + B - 4}{8}, \quad (\text{S44})$$

where we used the short-hand notation

$$\cos(2\theta) = \frac{\bar{\omega}_r^2 - \Omega_q^2}{\sqrt{(\bar{\omega}_r^2 - \Omega_q^2)^2 + 16G^2\bar{\omega}_r\bar{\omega}_q}}, \quad (\text{S45})$$

$$A = \frac{(\omega_+ + \omega_- - \bar{\omega}_r^2)(\omega_+ - \omega_-)}{\bar{\omega}_r\omega_+\omega_-} \quad (\text{S46})$$

$$B = \frac{(\omega_+ + \omega_- + \bar{\omega}_r^2)(\omega_+ + \omega_-)}{\bar{\omega}_r\omega_+\omega_-}. \quad (\text{S47})$$

For small  $g$  the result for  $\langle a^\dagger a \rangle$  can be further simplified to the expression given in Eq. (9) in the main text.

## ULTRASTRONG COUPLING PERTURBATION THEORY

In this section we summarize the details of the perturbation theory used to describe the ground state properties in the ultrastrong coupling regime  $g > \bar{\omega}_r, \bar{\omega}_q$ . In this regime the full Hamiltonian can be written as  $H = H_0 + H_1$ , where

$$H_0 = \hbar\bar{\omega}_r a^\dagger a + \hbar g(a^\dagger + a)S_x + \hbar D S_x^2, \quad (\text{S48})$$

and  $H_1 = \bar{\omega}_q S_z$ . We see that  $H_0$  commutes with  $S_x$  and it can be diagonalized by a *Lang-Firsov* transformation,  $\tilde{H}_0 = U^\dagger H_0 U$ , where

$$U = \exp(-\gamma(a^\dagger - a)S_x), \quad \gamma = \frac{g}{\bar{\omega}_r}. \quad (\text{S49})$$

We obtain

$$\tilde{H}_0 = \hbar\bar{\omega}_r a^\dagger a + \hbar \underbrace{\left(D - \frac{g^2}{\bar{\omega}_r}\right)}_{\delta} S_x^2. \quad (\text{S50})$$

Therefore, in this new frame the eigenstates are  $|s, m_x\rangle|n\rangle$ , where  $s$  is the total spin quantum number,  $m_x$  is the spin projection along  $x$  and  $|n\rangle$  is the number state of the resonator mode. The corresponding energies are  $E_{m_x, n} = \hbar\bar{\omega}_r n + \hbar\delta m_x^2$ . After transforming back into the original frame, we obtain the following set of eigenstates of  $H_0$ ,

$$|\Psi_{s, m_x, n}\rangle = U|s, m_x\rangle|n\rangle = \exp(-\gamma(a^\dagger - a)S_x)|s, m_x\rangle|n\rangle. \quad (\text{S51})$$

### Perturbation theory

For  $\delta \rightarrow 0$  the eigenspectrum of  $H_0$  consists of a set of highly degenerate manifolds separated by multiples of  $\hbar\bar{\omega}_r$ . This degeneracy is lifted by the qubit Hamiltonian  $H_1$  and in the following we are interested in the effect of  $H_1$  on the ground-state manifold spanned by the states with  $n = 0$ . To do so we need the matrix elements

$$\langle \Psi_{s, m'_x, n} | H_1 | \Psi_{s, m_x, 0} \rangle = \hbar\bar{\omega}_q e^{-\frac{\gamma^2(m_x - m'_x)^2}{2}} \frac{\gamma^n (m'_x - m_x)^n}{\sqrt{n!}} \langle s, m'_x | S_z | s, m_x \rangle, \quad (\text{S52})$$

where

$$\langle s, m'_x | S_z | s, m_x \rangle = \frac{1}{2} \left[ \delta_{m'_x, m_x+1} \sqrt{s(s+1) - m_x(m_x+1)} + \delta_{m'_x, m_x-1} \sqrt{s(s+1) - m_x(m_x-1)} \right]. \quad (\text{S53})$$

To first order in  $H_1$  we then obtain a tunneling between neighboring  $m_x$  states, i.e.,

$$\langle \Psi_{s, m'_x, 0} | H_1 | \Psi_{s, m_x, 0} \rangle = \hbar\bar{\omega}_q e^{-\frac{\gamma^2}{2}} \langle s, m'_x | S_z | s, m_x \rangle. \quad (\text{S54})$$

By introducing effective spin operators  $\tilde{S}_k$  via the relation

$$\langle \Psi_{s', m'_x, 0} | \tilde{S}_k | \Psi_{s, m_x, 0} \rangle = \langle s', m'_x | S_z | s, m_x \rangle \quad (\text{S55})$$

we can write the first order correction to the effective ground state Hamiltonian as

$$H_{\text{eff}}^{(1)} = \hbar\bar{\omega}_q e^{-\frac{\gamma^2}{2}} \tilde{S}_z. \quad (\text{S56})$$

To second order in  $\bar{\omega}_q$  the states in the ground state manifold are coupled to higher  $n$ -states, which are separated by an energy  $\hbar\bar{\omega}_r n$ . These processes can be treated in second order perturbation theory and we obtain

$$H_{\text{eff}}^{(2)} = \sum_{s=0}^{N/2} \sum_{m_x, m'_x=-s}^s M(s, m'_x, m_x) |\Psi_{s, m'_x, 0}\rangle \langle \Psi_{s, m_x, 0}|, \quad (\text{S57})$$

where

$$M(s, m'_x, m_x) = - \sum_{n=1}^{\infty} \frac{\langle \Psi_{s, m'_x, 0} | H_1 | \Psi_{s, m_x + 1, n} \rangle \langle \Psi_{s, m_x + 1, n} | H_1 | \Psi_{s, m_x, 0} \rangle}{(2m_x + 1)\hbar\delta + \hbar\bar{\omega}_r n} \quad (\text{S58})$$

$$- \sum_{n=1}^{\infty} \frac{\langle \Psi_{s, m'_x, 0} | H_1 | \Psi_{s, m_x - 1, n} \rangle \langle \Psi_{s, m_x - 1, n} | H_1 | \Psi_{s, m_x, 0} \rangle}{(-2m_x + 1)\hbar\delta + \hbar\bar{\omega}_r n}. \quad (\text{S59})$$

As a main contribution from this second order correction we obtain a diagonal term, which for small  $\delta$  is approximately given by

$$M(s, m_x, m_x) = \frac{\hbar\bar{\omega}_q^2}{2\bar{\omega}_r} e^{-\gamma^2} [m_x^2 - s(s+1)] \times \sum_{n=1}^{\infty} \frac{\gamma^{2n}}{n!n}. \quad (\text{S60})$$

For  $\gamma \gtrsim 2$  the remaining sum is reasonably well approximated by

$$\sum_{n=1}^{\infty} \frac{\gamma^{2n}}{n!n} \simeq \frac{e^{\gamma^2}}{\gamma^2}, \quad (\text{S61})$$

and we obtain the second order contribution

$$H_{\text{eff}}^{(2)} = \frac{\hbar\bar{\omega}_q^2\bar{\omega}_r}{2g^2} [\tilde{S}_x^2 - \tilde{S}^2]. \quad (\text{S62})$$

Since these energy shifts are not exponentially suppressed,  $H_{\text{eff}}^{(2)}$  dominates over the first order corrections and determines the basic ordering of the energy levels. In particular, this result shows that for given  $m_x$  the maximal angular momentum states with  $s = N/2$  are lowest in energy. Since  $H$  preserves the total angular momentum, it is enough to evaluate the low excitation properties within this  $s = N/2$  manifold.

*Remarks:* In the result given in Eq. (S62) we have neglected second order contributions which lead to transitions  $m_x \rightarrow m_x \pm 2$ . The corresponding matrix elements scale like

$$M(s, m_x, m_x \pm 2) \sim e^{-\gamma^2} \sum_{n=1}^{\infty} \frac{(-\gamma^2)^n}{n!n} \sim \log(\gamma) e^{-\gamma^2}. \quad (\text{S63})$$

Therefore, for large  $\gamma$  these contributions are exponentially small compared other terms in  $H_{\text{eff}}^{(1)}$  and  $H_{\text{eff}}^{(2)}$  and can be neglected.

Note that in addition to the energy correction we also obtain a correction to the state vectors, which are more precisely given by

$$|\Psi_{s, m_x, 0} \rangle \simeq |\Psi_{s, m_x, 0} \rangle^{(0)} + |\Psi_{s, m_x, 0} \rangle^{(1)}, \quad (\text{S64})$$

where  $|\Psi_{s, m_x, 0} \rangle^{(0)}$  are the unperturbed states introduce above and

$$|\Psi_{s, m_x, 0} \rangle^{(1)} = -\hbar\bar{\omega}_q e^{-\frac{\gamma^2}{2}} \sum_{m'_x=-N/2}^{N/2} \sum_{n=1}^{\infty} \frac{\gamma^n (m'_x - m_x)^n}{\sqrt{n!}} \frac{\langle s, m'_x | S_z | s, m_x \rangle}{(m'^2_x - m_x^2)\hbar\delta + \hbar\bar{\omega}_r n} |\Psi_{s, m'_x, n} \rangle^{(0)}, \quad (\text{S65})$$

are the corrections to first order in  $H_q$ . For most quantities these corrections are not essential, but they can lead to additional contributions in the expectation values, that are not taken into account in the analysis in the main text. A significant correction occurs, for example, for the qubit polarization

$$\langle \Psi_{N/2, 0, 0} | S_z | \Psi_{N/2, 0, 0} \rangle \approx -\frac{N(N+2)}{4} \frac{\bar{\omega}_q \bar{\omega}_r}{g^2}, \quad (\text{S66})$$

which according to  $H_{\text{eff}}$  would decay exponentially at large  $g$ . Also the photon number decays for extremely large  $g$  algebraically, namely

$$\langle \Psi_{N/2, 0, 0} | a^\dagger a | \Psi_{N/2, 0, 0} \rangle \approx \frac{N(N+2)}{8} \frac{\bar{\omega}_r^4 \bar{\omega}_q^2}{g^6}, \quad (\text{S67})$$

which, however, is invisible in figure 2 of the main text.

Finally, we emphasize that the validity of the effective Hamiltonian  $H_{\text{eff}}$  requires that for each  $n$  the matrix elements given in Eq. (S52) are small compared to the energy difference  $\hbar\bar{\omega}_r n$ . The matrix elements are exponentially suppressed for small  $n$  and reach maximal value for  $n_0 \approx \gamma^2$ . Therefore, the validity of the perturbation theory is restricted to parameters

$$\frac{\sqrt{s(s+1)}\bar{\omega}_q}{2} < \frac{g^2}{\bar{\omega}_r}. \quad (\text{S68})$$

---

[S1] M. H. Devoret, *Quantum Fluctuations in Electrical Circuits, Les Houches, Session LXIII*, (1997).

[S2] M. H. Devoret, S. Girvin, and R. Schoelkopf, Circuit-QED: How strong can the coupling between a Josephson junction atom and a transmission line resonator be?, *Ann. Phys. (NY)* **16**, 767 (2007).

[S3] J. Bourassa, J. M. Gambetta, A. A. Abdumalikov, O. Astafiev, Y. Nakamura, and A. Blais, Ultrastrong coupling regime of cavity QED with phase-biased flux qubits, *Phys. Rev. A* **80**, 032109 (2009).

[S4] P. Nataf and C. Ciuti, Vacuum Degeneracy of a Circuit QED System in the Ultrastrong Coupling Regime, *Phys. Rev. Lett.* **104**, 023601 (2010).

[S5] B. Peropadre, D. Zueco, D. Porras, and J. J. Garcia-Ripoll, Nonequilibrium and Nonperturbative Dynamics of Ultrastrong Coupling in Open Lines, *Phys. Rev. Lett.* **111**, 243602 (2013).

[S6] P. Forn-Diaz, J. J. Garcia-Ripoll, B. Peropadre, M. A. Yurtalan, J.-L. Orgiazzi, R. Belyansky, C. M. Wilson, and A. Lupascu, arXiv:1602.00416 (2016).

[S7] F. Yoshihara, T. Fuse, S. Ashhab, K. Kakuyanagi, S. Saito, and K. Semba, arXiv:1602.00415 (2016).

[S8] T. P. Orlando, J. E. Mooij, L. Tian, C. H. van der Wal, L. S. Levitov, S. Lloyd, and J. J. Mazo, Superconducting persistent-current qubit, *Phys. Rev. B* **60**, 15398 (1999).

[S9] T. Holstein and H. Primakoff, Field Dependence of the Intrinsic Domain Magnetization of a Ferromagnet, *Phys. Rev.* **58**, 1098 (1940).

[S10] C. Emary and T. Brandes, Chaos and the quantum phase transition in the Dicke model, *Phys. Rev. E* **67**, 066203 (2003).